

ORIGINAL ARTICLE

Prognostic serum miRNA biomarkers associated with Alzheimer's disease shows concordance with neuropsychological and neuroimaging assessment

L Cheng^{1,2}, JD Doecke^{3,4}, RA Sharples^{1,2}, VL Villemagne^{5,6,7}, CJ Fowler⁷, A Rembach⁷, RN Martins⁸, CC Rowe^{5,6}, SL Macaulay⁴, CL Masters⁷ and AF Hill^{1,2}, for the Australian Imaging, Biomarkers and Lifestyle (AIBL) Research Group

There is no consensus for a blood-based test for the early diagnosis of Alzheimer's disease (AD). Expression profiling of small non-coding RNA's, microRNA (miRNA), has revealed diagnostic potential in human diseases. Circulating miRNA are found in small vesicles known as exosomes within biological fluids such as human serum. The aim of this work was to determine a set of differential exosomal miRNA biomarkers between healthy and AD patients, which may aid in diagnosis. Using next-generation deep sequencing, we profiled exosomal miRNA from serum ($N=49$) collected from the Australian Imaging, Biomarkers and Lifestyle Flagship Study (AIBL). Sequencing results were validated using quantitative reverse transcription PCR (qRT-PCR; $N=60$), with predictions performed using the Random Forest method. Additional risk factors collected during the 4.5-year AIBL Study including clinical, medical and cognitive assessments, and amyloid neuroimaging with positron emission tomography were assessed. An AD-specific 16-miRNA signature was selected and adding established risk factors including age, sex and apolipoprotein $\epsilon 4$ (APOE $\epsilon 4$) allele status to the panel of deregulated miRNA resulted in a sensitivity and specificity of 87% and 77%, respectively, for predicting AD. Furthermore, amyloid neuroimaging information for those healthy control subjects incorrectly classified with AD-suggested progression in these participants towards AD. These data suggest that an exosomal miRNA signature may have potential to be developed as a suitable peripheral screening tool for AD.

Molecular Psychiatry advance online publication, 28 October 2014; doi:10.1038/mp.2014.127

INTRODUCTION

Alzheimer's disease (AD) is characterised by the accumulation of the beta-amyloid peptide ($A\beta$) that is proteolytically cleaved from the amyloid precursor protein (APP).¹ Positron emission tomography (PET) scanning using carbon-11-labelled Pittsburgh compound B (¹¹C-PiB) to image $A\beta$ has shown that $A\beta$ deposition is a slow pathological process that occurs over a period of two decades.² Thus, the long preclinical phases before the onset of dementia presents a challenge for early diagnosis and stratification of AD patients. Progress in developing methods to characterise AD has been assisted by recruiting cohorts of healthy aged individuals and those with AD, which have produced promising diagnostic/prognostic methods such as $A\beta$ imaging using PET² and the measurement of $A\beta$ levels in cerebrospinal fluid (CSF).³ Although these methods have shown excellent diagnostic/prognostic accuracy for AD, the high costs of PET and invasive nature of CSF collection currently preclude their utility for routine clinical testing. Therefore, a non-invasive and high-throughput blood-based test is required for improved population-based screening and patient care in order to refer patients for further examination. In addition, with numerous drug trials aiming to treat AD, a blood-based test would be ideal to

enrich cohorts of AD cases followed by monitoring the potential benefits and side effects of therapeutic drugs.

MicroRNA (miRNA) are non-coding RNA species of 22 nucleotides that are transcribed in all tissues and cells.⁴ The function of miRNA are to bind complementary sites of the 3' untranslated region of their mRNA targets resulting in downregulation of gene expression.⁵ miRNAs can be released into the extracellular environment by binding to RNA-binding proteins or through secretion in cell-derived plasma microvesicles such as exosomes.^{6–8} The profile of miRNA expression levels when sampled in the extracellular environment can therefore reflect the physiological state of the biological system. Profiles of deregulated miRNA isolated from plasma and serum^{7,9} have been generated and suggest that these have diagnostic potential for human disease.

Exosomes isolated from serum have been shown to be highly enriched in miRNA and a number of specific miRNA genes are specifically found in exosomes.^{10,11} The value of analysing enriched exosomal miRNA is greater than that of non-exosomal miRNA, as miRNA is essentially diluted in circulating blood that results in an increased signal-to-noise ratio. This suggests that exosomal miRNA in the body can be analysed and provide a disease-specific diagnostic picture that can be applied to predict the onset of AD and/or monitor the various stages of AD.

¹Department of Biochemistry and Molecular Biology, The University of Melbourne, Melbourne, VIC, Australia; ²Bio21 Molecular Science and Biotechnology Institute, The University of Melbourne, Melbourne, VIC, Australia; ³CSIRO Digital Productivity Flagship/The Australian E-Health Research Centre, Herston, QLD, Australia; ⁴CSIRO Food and Nutrition Flagship, Melbourne, VIC, Australia; ⁵Department of Nuclear Medicine and Centre for PET, Austin Health, Melbourne, VIC, Australia; ⁶Department of Medicine, Austin Health, Melbourne, VIC, Australia; ⁷Florey Institute, Melbourne, VIC, Australia and ⁸Faculty of Computing Health and Science, Centre of Excellence for Alzheimer's Disease Research and Care, School of Medical Sciences, Edith Cowan University, Joondalup, WA, Australia. Correspondence: Professor AF Hill, Department of Biochemistry and Molecular Biology, Bio21 Molecular Science and Biotechnology Institute, The University of Melbourne, 30 Flemington Road, Parkville, VIC 3010, Australia.

E-mail: a.hill@unimelb.edu.au

Received 23 May 2014; revised 10 August 2014; accepted 25 August 2014

Recent developments in high-throughput next-generation sequencing (NGS) have enabled profiling of miRNA levels in biological fluids as a viable diagnostic method for biomarker discovery.¹² Previously, we observed that miRNA were significantly enriched in exosomes isolated from serum compared with non-exosomal cell-free samples.¹¹ The isolation of exosomes typically involves up to 4 h of sequential ultracentrifugation steps.^{6,7,10,11} Increased purity of exosomes devoid of other extracellular vesicles can be further isolated by density gradients.¹³ Isolating a pure population of exosomes is essential when investigating functionality and biogenesis but may not be of high priority in biomarker studies. It is more desirable for a biomarker to be specific, sensitive and reproducible. Thus, we also considered more efficient methods of exosome isolation by comparing miRNA exosomal profiles isolated by a commercial exosomal isolation kit with profiles from serum exosomes isolated by the ultracentrifuge.¹¹ We found that the miRNA profiles obtained from the Norgen Biotek Plasma/Serum Exosomal RNA kit were similar to profiles extracted from characterised exosomes isolated by the ultracentrifugation method.¹¹ In order to develop a biomarker, one priority for this study was to produce a method that could be reproducible across any laboratory or diagnostic clinic that may not have access to an ultracentrifuge. The use of the commercial kit would allow reproducibility across collection sites including the ability to efficiently process large number of samples.

In this study, we profiled exosomal miRNA to determine a set of differential exosomal miRNA biomarkers between healthy and AD patients through unbiased NGS followed by quantitative reverse transcription PCR (qRT-PCR) validation. Human serum was collected by the Australian Imaging, Biomarkers and Lifestyle Group (AIBL) Flagship Study of Aging, which is a large longitudinal study committed to discovering the biomarkers and lifestyle factors that determine the prevalence of AD.^{14–16} From healthy and AD participants in the AIBL cohort, we identified an AD-specific 16-miRNA signature from the NGS training set, which was validated using qRT-PCR to predict AD.

MATERIALS AND METHODS

Participants

Participants were selected from the Melbourne arm of AIBL (www.aibl.csiro.au) and divided into three groups: healthy controls (HC), mild cognitive impairment (MCI) and AD based on the established criteria from the National Institute of Neurological and Communicative Disorders and Stroke–Alzheimer's Disease and Related Disorders Association (NINCDS–ADRD)¹⁷, which has been described in detail elsewhere.¹⁶ Blood samples were collected from all participants (fasting) from whole-blood venepuncture into Sarstedt s-monovette serum-gel 7.5-ml tubes (Sarstedt, Mawson Lakes, SA, Australia). Serum-gel tubes were processed within 2 h of collection and serum was snap-frozen in liquid nitrogen. In the discovery sample set, serum from 49 participants (HC, 23; MCI, 3 and AD, 23) were collected for deep sequencing and serum from 60 participants (HC, 36; MCI, 8 and AD, 16) were collected for validation. All individuals included were assessed for full blood pathology (Melbourne Health and PathWest Laboratory Medicine), apolipoprotein $\epsilon 4$ (APOE $\epsilon 4$) genotyping and assessment of cognitive functions (mini-mental state examination) at the time of collection.¹⁶ Of these, 83 (23 in the discovery set and 60 in the validation set) participants underwent A β neuroimaging with PiB–PET. A β burden was expressed as ¹¹C–PiB-standardised uptake value ratio (PiB–SUVR) as previously described.² Participant data from both baseline and 54-month time points were available for analyses. Informed consent was obtained from all AIBL participants and ethics were approved by the institutional ethics committees of Austin Health and St Vincent's Health.

Small RNA deep sequencing and qRT-PCR validation

Serum exosomal RNA was isolated by using the Plasma/Serum Exosomal RNA Isolation Kit (formerly no. 49200, repackaged to no. 51000 Plasma/Serum Circulating and Exosomal RNA Purification Mini Kit; Norgen Biotek, ON, Canada) from 1 ml serum per participant following the manufacturers' protocol. The total exosomal RNA yield, composition and quality were

analysed by the Agilent 2100 Bioanalyser using the Small RNA kit (Agilent, Agilent Technologies, Santa Clara, CA, USA). Exosomal RNA was converted into cDNA libraries using the Ion Total RNA-Seq Kit V2 (Life Technologies, Mulgrave, VIC, Australia) and prepared for sequencing as described previously.¹⁸ Pooled libraries with unique barcodes were loaded on 318 sequencing chips and run on the Ion Torrent Personal Genome Machine (Life Technologies).¹⁸ The sequences were then assessed for quality and primer-adaptor sequences were trimmed by the Torrent Suite software (version 3.4.1; Life Technologies), followed by alignment to the human reference genome (HG19). The trimmed and aligned data was transferred to Partek Genomics Suite (Partek, Singapore) and mapped to known miRNA using miRBase version 20. Bioinformatics analysis and differential expression was performed using Partek Genomics Suite. The panel of candidate miRNA found highly associated with AD (including positive and negative controls) were used for validation on a new set of serum samples collected from AIBL. Using the GENorm method as implemented in the Bioconductor package NormqPCR, a similar algorithm¹⁹ was applied on the deep sequencing data to identify an endogenous normaliser in these samples (Supplementary Figure 1). Hsa-miR-451 was the most stable endogenous representative, with the lowest 'M' score. Other potential endogenous controls include hsa-miR-223-3p, hsa-miR-486-5p and hsa-miR-191-5p. Serum samples for the validation study were also spiked with synthetic *Caenorhabditis elegans* miR-39 (cel-miR-39, Qiagen, Chadstone, VIC, Australia) during exosomal RNA extraction to monitor extraction efficiency and for normalisation purposes. Upon processing of the serum samples as above, 1 ng of exosomal miRNA was converted to cDNA (TaqMan MicroRNA Reverse Transcription Kit, Applied Biosystems, Mulgrave, VIC, Australia) according to the manufacturers' protocol with a primer pool containing 23 miRNA assays (TaqMan microRNA assays, 5x, Applied Biosystems). cDNA samples were pre-amplified (TaqMan PreAmp Master Mix Kit, Applied Biosystems) and qRT-PCR (TaqMan Fast Advanced Master Mix, Applied Biosystems) was performed using individual miRNA assays (TaqMan microRNA assays, 20x, Applied Biosystems) and run on the ViiA 7 Real-Time PCR System (Life Technologies) across a 384-well format. Reverse transcription and pre-amplification no template controls using primer pools and individual assays were also prepared to ensure there was no background amplification of miRNA assays. Raw C_t data was uploaded to DataAssist (Applied Biosystems) to calculate delta C_t (ΔC_t) using normalisation controls (cel-miR-39 and hsa-miR-451), which were then used for further statistical analysis.

Statistical analysis

To analyse the deep sequencing data, the number of reads of each miRNA were normalised to reads per million across all samples. Low abundant miRNAs with < 50 read counts across all samples were removed thus, high abundant miRNAs were analysed in this study. Initial statistical analysis of miRNA expression changes was performed using the Partek Genomics Suite. Selection of miRNAs was based upon analysis of variance (ANOVA) comparing HC and AD groups (clinical classification at the time of collection). Probability values were adjusted for multiple testing using the false discovery rate method. Significant changes in miRNA expression were expressed in fold change (\log_2) and defined as P (AD vs HC) ≤ 0.05 , P (AD, MCI and HC) ≤ 0.05 and ± 1.2 -fold change. Generalised linear modelling was performed to assess each miRNA chosen from the initial analyses adjusted for age, gender and APOE $\epsilon 4$ allele status. Further classification (discovery data set) and prediction (validation data set) analyses was performed using Random Forest analyses. From these models, sensitivity and specificity, and related statistics were calculated. All statistical analyses were performed using the R statistical environment, version 3.02.

RESULTS

Exosomal miRNA discovery set analyses

The characteristics of the participants included in this study are shown in Table 1. The prevalence of APOE $\epsilon 4$ was significantly higher in the AD group compared with HCs ($P=0.006$). AD participants performed significantly worse in the mini-mental state examination ($P=0.006$) and obtained low clinical dementia ratings ($P<0.0001$) and composite scores (composite score 1: $P<0.0001$ and composite score 2: $P<0.0001$) as expected. Deep sequencing of the exosomal RNA extracted from serum samples was performed and sequences were mapped to miRBase

version 20. Approximately half of the reads obtained (43%) from small RNA sequencing corresponded with miRNA sequences (Supplementary Table 1). Overall, the sample cohort mapped to 1419 known human miRNA sequences (Supplementary Table 2). Following normalisation of reads and performing ANOVA analyses, 17 miRNA were found to be significantly deregulated (P ANOVA (AD vs HC) ≤ 0.05 , P ANOVA (AD, MCI and HC) ≤ 0.05 and ± 1.2 -fold change; Figure 1); 14 miRNA were found to be upregulated (hsa-miR-361-5p, hsa-miR-30e-5p, hsa-miR-93-5p, hsa-miR-15a-5p, hsa-

miR-143-3p, hsa-miR-335-5p, hsa-miR-106b-5p, hsa-miR-101-3p, hsa-miR-424-5p, hsa-miR-106a-5p, hsa-miR-18b-5p, hsa-miR-3065-5p, hsa-miR-20a-5p and hsa-miR-582-5p) and three miRNA were found to be downregulated (hsa-miR-1306-5p, hsa-miR-342-3p and 15b-3p; Table 2). Upon post adjustment of age, APOE $\epsilon 4$ allele status and sex (generalised linear modelling), the majority of miRNA remained statistically significant upon contrasting within all attribute groups (AD, MCI and HC) and between AD and HC (Table 2). Although there were only three MCI participants in the study, MCI occurs in the general population, and should be included in the machine learning model, which can handle the use of multiple classification groups.

Partitioning Around Medoids clustering of the 17 miRNA revealed two main clusters: one for those miRNAs upregulated in AD and the other for those downregulated in AD. Further investigation of these identified four clusters (Figure 2a), with stepwise increases in miRNA expression across APOE $\epsilon 4$ allele carriers and clinical classification (Figure 2b). Delineation into miRNA cluster averages showed clear associations with APOE $\epsilon 4$ allele status (Figure 2c), confirming the stepwise increases shown by assessing miRNA by cluster. Variable selection using Random Forest analysis (Figure 2d) defined hsa-miR-1306-5p as contributing more towards clinical classification than age, indicating this miRNA as vitally important in class separation.

Receiver operating characteristic analysis statistics for each miRNA marker of the discovery phase are shown in Supplementary Table 4. The receiver operating characteristic analyses were performed using the raw sequence count data to estimate the performance of each miRNA to predict AD. Criterion cut points were chosen by taking the closest point on the curve to the top left corner of the receiver operating characteristic curve, approximating the most optimum performance for each marker. Independently, the miRNAs were displayed between 35% and 100% sensitivity and specificity, respectively. Similar to the Random Forest model, hsa-miR-1306-5p showed the greatest combined, sensitivity and specificity (87.5% and 70%, respectively; $P = 0.0008$).

qRT-PCR validation set analyses

All participants in the validation set ($n = 60$, Table 1) underwent full assessment including PiB-PET neuroimaging performed at

Table 1. Demographics and clinical makeup of discovery and validation set

Discovery set	HC	MCI	AD	P-value ^a
N	23	3	23	
Age (mean \pm s.d.)	73.07 (7.57)	76.91 (4.4)	78.89 (7.33)	0.034
Gender (F/M)	10/13	1/2	13/9	0.484
APOE $\epsilon 4$ (-ve/+ve)	18/5	1/2	7/15	0.006
MMSE (mean \pm s.d.)	29 (1.25)	23 (5.66)	15 (8.66)	< 0.0001
Composite score 1 (mean \pm s.d.)	0.26 (0.73)	-2.04 (0.80)	-2.41 (0.25)	< 0.0001
Composite score 2 (mean \pm s.d.)	0.10 (1.10)	-1.79 (1.18)	-2.10 (0.90)	< 0.0001
Validation set	HC	MCI	AD	P-value ^a
N	36	8	16	
Age (mean \pm s.d.)	78.55 (6.52)	78.91 (6.3)	78.29 (7.55)	0.963
Gender (F/M)	21/14	4/4	10/5	0.737
APOE $\epsilon 4$ (-ve/+ve)	27/8	6/2	2/13	0.0001
MMSE (mean \pm s.d.)	30 (1.08)	29 (2.03)	21 (8.14)	< 0.0001
Composite score 1 (mean \pm s.d.)	0 (0.59)	-1.16 (0.65)	-2.02 (0.65)	< 0.0001
Composite score 2 (mean \pm s.d.)	0 (0.91)	-0.63 (0.7)	-1.64 (0.4)	0.046

Abbreviations: AD, Alzheimer's disease; APOE $\epsilon 4$, apolipoprotein $\epsilon 4$; F, female; HC, healthy control; M, male; MCI, mild cognitive impairment; MMSE, mini-mental state examination. ^aCompared with healthy controls.

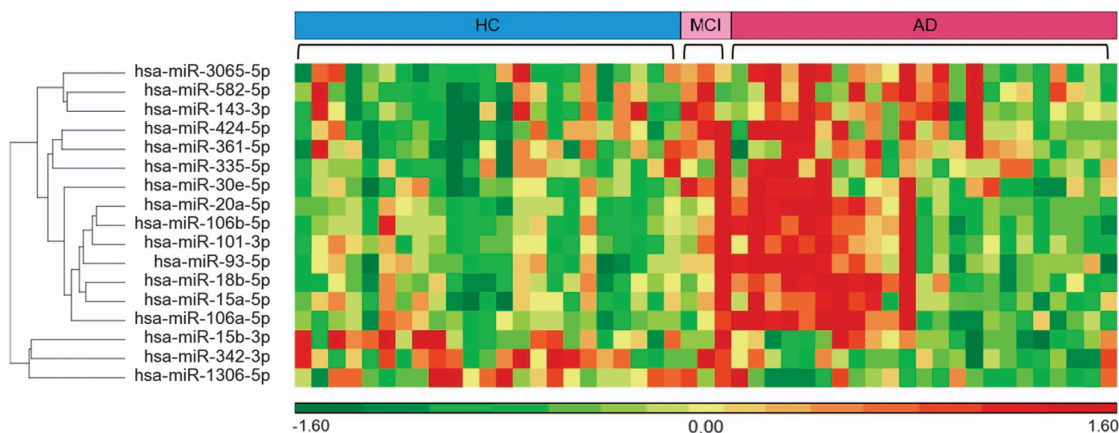


Figure 1. Hierarchical clustering of differentially expressed exosomal microRNA (miRNA) biomarkers obtained from healthy controls (HC) and participants with Alzheimer's disease (AD). Using the deep sequencing data obtained from the discovery set, hierarchical clustering was performed using Partek Genomics Suite on significantly differentially expressed miRNA using Euclidean average linkage by miRNA. Seventeen miRNAs were found to be significantly deregulated (P (AD vs HC) ≤ 0.05 , P (AD, MCI and HC) ≤ 0.05 and ± 1.2 -fold change). There are two major nodes of the dendrogram. Node 1 contains 15 miRNAs that were found to be upregulated (hsa-miR-361-5p, hsa-miR-30e-5p, hsa-miR-93-5p, hsa-miR-15a-5p, hsa-miR-143-3p, hsa-miR-335-5p, hsa-miR-106b-5p, hsa-miR-101-3p, hsa-miR-424-5p, hsa-miR-106a-5p, hsa-miR-18b-5p, hsa-miR-3065-5p, hsa-miR-20a-5p, hsa-miR-3065-5p and hsa-miR-582-5p). Node 2 contains three miRNAs that were found to be downregulated (hsa-miR-1306-5p, hsa-miR-342-3p and hsa-miR-15b-3p; Table 2). Patient samples were arranged by attribute (HC, MCI and AD).

Table 2. Number of reads obtained from deep sequencing data per miRNA across each clinical classification

Cluster	miRNA	HC	MCI	AD	Fold change	P-value	P-value (GLM) ^a			
		Mean RPM (s.d.)	Mean RPM (s.d.)	Mean RPM (s.d.)		ANOVA	All groups (unadjusted)	All groups (adjusted)	HC vs AD (unadjusted)	HC vs AD (adjusted)
1	hsa-miR-30e-5p	85.38 (18.81)	160.39 (34.93)	111.26 (35.59)	1.3	1.10E-04	0.02	0.03	0.01	0.01
1	hsa-miR-101-3p	75.14 (20.29)	164.98 (118.45)	107.38 (63.26)	1.43	0.01	0.1	0.44	0.07	0.01
1	hsa-miR-15a-5p	2472.22 (769.66)	4168.34 (2182.56)	3254.91 (1407.36)	1.32	0.02	0.05	0.13	0.04	0.01
1	hsa-miR-20a-5p	1774.54 (484.33)	3191.99 (1824.21)	2818.21 (1568.42)	1.59	9.53E-03	0.02	0.1	0.02	0.02
1	hsa-miR-93-5p	2577 (601.67)	3941.08 (1307.43)	3389.06 (1236.83)	1.32	9.26E-03	0.03	0.18	0.03	0.02
1	hsa-miR-106b-5p	658.56 (209.64)	1244.95 (693.21)	900.7 (462.92)	1.37	0.02	0.09	0.4	0.07	0.01
1	hsa-miR-18b-5p	64.7 (20.93)	105.09 (53.34)	96.48 (42.46)	1.49	6.85E-03	0.01	0.05	0.01	0.03
1	hsa-miR-106a-5p	318.95 (84.52)	396.55 (130.17)	450.94 (218.61)	1.41	0.03	0.04	0.23	0.05	0.01
2	hsa-miR-1306-5p	46.72 (22.26)	49.45 (14.6)	30.72 (15.19)	0.66	0.01	0.01	0.05	0.01	0.04
3	hsa-miR-3065-5p ^b	34.45 (23.2)	54.11 (7.36)	52.86 (27.71)	1.53	0.04	0.01	0.1	0.01	0.02
3	hsa-miR-582-5p	15.84 (10.82)	29.42 (16.55)	25.41 (12.43)	1.6	0.02	0.01	0.06	0.01	0.02
3	hsa-miR-143-3p	111.69 (53.6)	181.94 (51.29)	149.21 (52.8)	1.34	0.02	0.02	0.07	0.02	0.03
3	hsa-miR-335-5p	162.37 (66.68)	324.52 (261.5)	220.19 (88.08)	1.36	0.01	0.04	0.03	0.02	0.01
3	hsa-miR-361-5p	92.54 (37.34)	168.95 (65.87)	115.56 (30.05)	1.25	2.26E-03	0.03	0.13	0.03	0.01
3	hsa-miR-424-5p	133.39 (52.13)	276.11 (70.43)	192.54 (76.59)	1.44	5.70E-04	0.01	0.03	0.01	0.01
4	hsa-miR-342-3p	1188.13 (340.76)	1652.05 (880.91)	915.22 (240.32)	0.77	1.04E-03	0.02	0.07	0.01	0.01
4	hsa-miR-15b-3p	163.91 (44.24)	188.67 (93.58)	135.28 (38.94)	0.83	0.04	0.04	0.04	0.03	0.01

Abbreviations: AD, Alzheimer's disease; ANOVA, analysis of variance; APOE ϵ 4, apolipoprotein ϵ 4; GLM, generalised linear modelling; HC, healthy control; MCI, mild cognitive impairment; miRNA, microRNA; qRT-PCR, quantitative reverse transcription PCR; RPM, reads per million. The average number of total reads obtained per sample was 780 371 (Supplementary Table 1). Reads were mapped to 1419 known mature miRNA using miRBase version 20. miRNA with < 50 reads across all samples were removed leaving 225 abundant miRNA for analysis. Raw reads (Supplementary Table 2) were normalised to RPM. RPM values for each sample are presented in Supplementary Table 3. ANOVA was performed by comparing cohort groups with HCs. ^aP-values are the result of generalised linear modelling pre- and post adjustment with age, sex and APOE ϵ 4 allele. miRBase version 20 accession numbers are presented in Supplementary Table 3. ^bHsa-miR-3065-5p was not used in the validation set as it was found to be undetectable using qRT-PCR.

baseline (before this study) and at 54 months (time of collection). Samples were spiked with synthetic cel-miR-39 as an external control and three highly abundant miRNA were run as endogenous controls (hsa-miR-451, hsa-miR-223-3p and hsa-miR-339-5p; Supplementary Table 5, Supplementary Figures 1 and 2). For quality control assurance and normalisation controls, cel-miR-39 was used as an external control and hsa-miR-451 was chosen as the endogenous control owing to its stable expression across all samples (Supplementary Figures 1 and 2). Previously, miR-451 was found to correlate with the degree of haemolysis.²⁰ We detected a maximum of 242 807 raw reads of hsa-miR-451 per 1 ml of sample compared with 1×10^6 copies per microlitre of plasma with no apparent haemolysis observed in Kirschner *et al.*²⁰ This indicates very little haemolysis in our samples most likely owing to the use of serum separator tubes.¹¹ Upon completion of the qRT-PCR assay, two samples did not display appropriate threshold levels of cel-miR-39 and hsa-miR-451, thus did not fulfil quality control measures and were removed. In addition, hsa-miR-3065-5p was found to be undetected ($C_t > 35$) in 40 samples. As qRT-PCR could not detect hsa-miR-3065-5p in all samples by qRT-PCR, this miRNA was removed from the list of biomarker candidates.

Model validation (Random Forest; Figure 2d), which incorporates all the 16 selected miRNA markers including age, gender and APOE ϵ 4 allele correctly diagnosed 13 out of 15 AD participants (sensitivity 87%; Table 3), and confirmed 27 out of 35 HC participants (specificity 77%; Table 3) when comparing participants 54-month clinical classification. Five clinically healthy participants (samples 7, 9, 16, 34 and 51, Table 3) classified as having AD using miRNA biomarkers, were found to have high A β burden in the brain upon PET neuroimaging with an PiB-SUVR > 1.5 across four time points of the AIBL longitudinal study, suggestive of higher risk of clinical manifestation of AD. Three female clinically healthy participants (samples 8, 17 and 39) were also classified as having AD using miRNA biomarkers, although showed low A β burden upon neuroimaging (PiB-SUVR < 1.5), they were APOE ϵ 4 carriers. Case-by-case information is presented in Table 3. Box plots of qRT-PCR data for each miRNA marker stratified by clinical classification are presented in Figure 3. Although a number of miRNA biomarkers show some overlap

between AD and HC groups, the final model incorporates all biomarkers to classify patients.

As our cohort size for MCI participants was small, we were unable to train our model to predict progression from HC to MCI or MCI to AD. Instead, we applied HC and AD thresholds to predict MCI participants in the validation set. Of the eight MCI participants at 54 months, two were classified as having AD (samples 27 and 53), whereas the remaining six were classified as HCs (Table 3). Further investigation using levels of neocortical A β burden as determined by PiB-PET imaging show that those MCI participants classified as having AD had high PiB-SUVR (> 1.5), suggesting that these participants may represent prodromal AD cases. Furthermore, three MCI participants who were classified as HC all had low PiB-SUVR and were negative for APOE ϵ 4, suggesting that they are not on an AD type dementia pathway. The remaining participants (samples 26, 28, 37, 49 and 29) incorrectly classified do not carry APOE ϵ 4 and were classified as HCs. Interestingly, sample 49, clinically classified as AD with a MMSE score of 10, displayed the highest PiB-SUVR score of 3.03 however, was classified as healthy using miRNA biomarkers (Table 3). This may indicate that the miRNA biomarkers are not suitable for late-stage AD diagnosis but are better predictors during early- to mid-stage AD during A β deposition.

DISCUSSION

The use of exosomes compared with cell-free or whole blood has a number of disease-specific advantages for diagnostic purposes. First, isolating the enriched miRNA in exosomes from biological samples of AD participants would remove insignificant circulating non-exosomal miRNA expressed in both AD and HC participants, thus providing a better performing predictive AD diagnosis. Second, miRNA originating from the brain have been shown to cross the endothelial cellular layers of the blood-brain barrier by transcytosis of exosomes across the endothelial layer in order to communicate between the brain and distant organs via biological fluids.²¹ Third, evidence has revealed that exosomes serve as a RNase-protective vesicle that shield miRNA from RNase-rich environments such as the circulatory system.²² Furthermore,

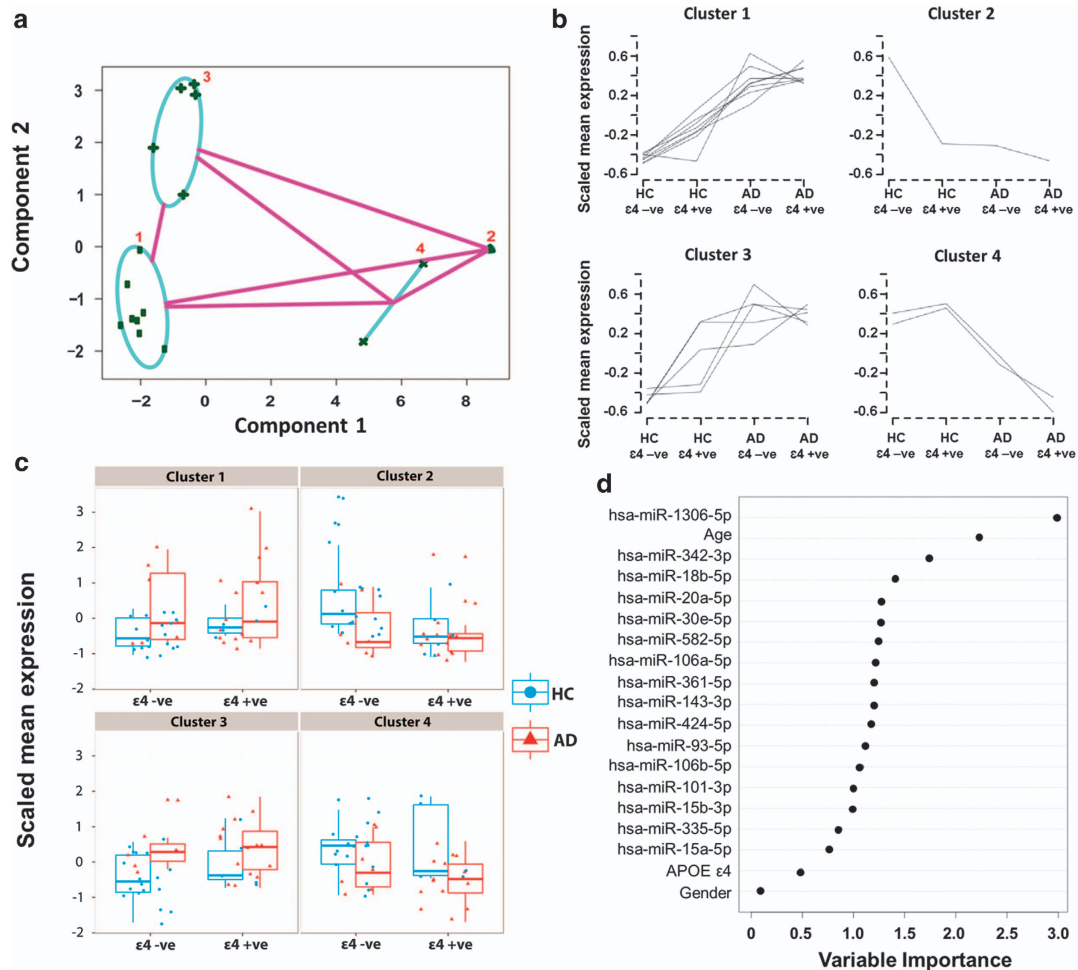


Figure 2. Clustering and random forest testing of correlated microRNA (miRNA) identified in healthy controls and participants with Alzheimer's disease (AD) within the discovery set. **(a)** Partitioning Around Medoids clustering of the 16 miRNAs used for validation. Two main clusters were found. One cluster included miRNAs upregulated in AD and the other one for those downregulated in AD. These two main clusters were broken into two further clusters each generating four clustered miRNA groups. **(b)** miRNA in clusters 1 and 3 show an increased mean expression across apolipoprotein $\epsilon 4$ (APOE $\epsilon 4$) allele and clinical classification. Cluster 2 and 4 represent a decrease in mean expression across (APOE $\epsilon 4$ allele and clinical classification). **(c)** Box plots of miRNA clusters displaying associations with APOE $\epsilon 4$ allele status and clinical classification. **(d)** Variable selection via Random Forest analyses ordered by importance of contribution towards clinical classification. The miRNAs found in each cluster are listed in Table 2.

specific packaging of miRNA into exosomes²³ and increased secretion of microvesicles into peripheral blood of cancer patients compared with healthy patients²⁴ suggests the importance of exosomes in the role of extracellular communication during disease. These factors allow the possibility of profiling disease-specific miRNA that are found enriched from exosomes.

Biomarker studies attempting to validate a large panel consisting of low abundant miRNAs or non-exosomal samples have resulted in moderate success during validation that resulted in changes of direction in expression between deep sequencing and qRT-PCR. Deep sequencing of Paxgene tubes generated a large panel of 180 deregulated miRNA in AD participants. Bioinformatics analysis using predictive tools was required to narrow the panel from 180 to 12 miRNA for validation, thus potentially losing disease specificity.²⁵ Using cell-free plasma, a 7-miRNA AD-associated signature was obtained from a total of 227 miRNA sequenced using Nanostring technology.²⁶ Although these studies demonstrate high accuracy, analysing exosomal miRNA would enrich disease-specific miRNA, which has shown relevancy when detecting central nervous system-related disorders. There have been a number of reports demonstrating the association of exosomes and neuronal proteins.^{11,27-29} We have

shown that exosomes are enriched with miRNA that target various neuronal-signalling pathways.¹¹ Upon comparing the levels of the 7-miRNA published in Kumar *et al.*,²⁶ we detected a significant enrichment of all seven miRNAs in exosomes within our study when comparing exosomal plasma samples with matching cell-free plasma samples (unpublished data).^{11,26} Nonetheless, it is difficult to compare the two studies that use different bio-fluids, sample processing methods and deep sequencing platforms. Further evidence has shown that the nuclear ribonucleoprotein, hnRNPA2B1, which contains a Prion-like domain and is involved in transport of mRNA in neurones, is implicated in specific loading of miRNA species into exosomes.²⁷ In addition, exosomes secreted into the extracellular environment are potentially involved in the pathogenesis of AD and Prion disease.²⁸⁻³⁰ We have shown that APP and its various fragments, including A β , are found in association with exosomes.²⁹

Many of the miRNA identified in this study have been shown to be implicated in AD pathogenesis using several mouse and cell models such as hsa-miR-101-3p, hsa-miR-20a-5p, hsa-miR-106b-5p, hsa-miR-15a-5p, hsa-miR-1306-5p, hsa-miR-15b-3p, 106b-5p, hsa-miR-106a-5p and hsa-miR-424-5p. In particular, hsa-miR-101 targets the 3' untranslated region of APP to significantly reduce

Table 3. Demographics, clinical makeup and clinical classification of participants of the validation set at baseline and 54 months including diagnosis by AD-associated exosomal miRNA signature

Sample no.	Age	Gender	APOE $\epsilon 4$	MMSE baseline	MMSE 54 m	PiB-SUVR baseline	PiB-SUVR 54 m	Clinical class. baseline	Clinical class. 54 m	miRNA class.
2	67	F	+	28	24	2.57	2.97	AD	AD	AD
46	73	F	+	25	21	2.04	NI	AD	AD	AD
50	59	F	+	23	25	1.59	NI	AD	AD	AD
40	69	F	+	30	26	2.6	NI	HC	AD	AD
48	78	M	+	30	16	2.25	2.39	HC	AD	AD
43	68	M	+	30	17	2.27	2.55	HC	AD	AD
5	75	F	+	27	21	2.64	2.82	MCI	AD	AD
4	84	M	+	26	23	2.44	2.48	MCI	AD	AD
58	77	F	+	27	26	2.06	NI	MCI	AD	AD
59	80	F	+	26	26	2.2	NI	MCI	AD	AD
55	76	F	+	27	27	2.1	2.31	MCI	AD	AD
47	84	F	+	22	2	2.55	NI	MCI	AD	AD
1	69	M	+	26	10	2.16	NI	MCI	AD	AD
3	81	F	-	29	29	1.06	1.13	HC	HC	HC
23	81	F	-	28	30	1.16	1.07	HC	HC	HC
12	81	F	-	30	30	1.26	1.24	HC	HC	HC
13	88	F	-	30	30	2.18	2.3	HC	HC	HC
19	80	M	-	30	29	2.03	2.41	HC	HC	HC
42	86	F	-	30	30	1.36	NI	HC	HC	HC
10	74	F	-	30	30	1.14	1.04	HC	HC	HC
11	63	M	-	29	28	1.36	1.31	HC	HC	HC
36	65	F	-	30	30	1.18	1.23	HC	HC	HC
32	72	F	-	26	29	1.35	1.61	HC	HC	HC
25	78	M	-	28	29	2.01	2.27	HC	HC	HC
18	78	F	-	29	28	1.87	NI	HC	HC	HC
15	76	F	-	28	26	1.79	2.03	HC	HC	HC
14	74	F	-	28	28	1.07	1.12	HC	HC	HC
22	76	F	-	28	30	1.13	NI	HC	HC	HC
20	76	M	-	26	29	1.27	1.25	HC	HC	HC
21	74	F	-	27	28	1.02	1.02	HC	HC	HC
35	67	F	-	29	30	1.08	1.04	HC	HC	HC
33	63	M	-	30	29	1.06	1.05	HC	HC	HC
45	61	F	-	29	30	1.11	1.22	HC	HC	HC
38	72	M	-	30	30	1.21	1.21	HC	HC	HC
44	71	M	-	30	30	1.22	1.3	HC	HC	HC
52	74	M	-	30	27	1.15	1.09	HC	HC	HC
54	77	M	-	30	30	1.18	1.3	HC	HC	HC
60	61	M	-	29	30	1.07	1.03	HC	HC	HC
56	76	F	-	29	28	1.19	1.39	HC	HC	HC
24	72	M	-	29	30	1.17	1.2	HC	HC	HC
9	73	F	+	29	29	1.69	1.75	HC	HC	AD
51	82	M	+	30	29	2.33	2.37	HC	HC	AD
7	79	F	+	28	27	2.07	NI	HC	HC	AD
16	74	M	+	29	30	1.35	1.52	HC	HC	AD
34	72	M	+	29	30	1.57	1.78	HC	HC	AD
17	76	F	+	30	30	1.11	1.08	HC	HC	AD
8	69	F	+	30	30	1.21	NI	HC	HC	AD
39	68	F	+	30	30	1.06	1.15	HC	HC	AD
27	70	M	+	26	28	2.05	2.56	MCI	MCI	AD
53	76	M	+	26	30	1.65	2.06	MCI	MCI	AD
57	82	F	-	29	29	1.1	1.22	MCI	MCI	HC
41	78	F	-	27	30	1.05	1.2	HC	MCI	HC
6	79	M	-	27	29	1	1.03	MCI	MCI	HC
26	68	F	-	30	29	1.4	NI	MCI	MCI	HC
28	78	M	-	28	25	2.16	2.38	MCI	MCI	HC
37	64	F	-	30	25	1.62	1.82	MCI	MCI	HC
49	82	M	-	20	10	3.04	3.03	AD	AD	HC
29	65	F	-	24	6	1.92	2.12	MCI	AD	HC

Abbreviations: AD, Alzheimer's disease; APOE $\epsilon 4$, apolipoprotein $\epsilon 4$; A β , beta-amyloid peptide; class., classification; F, female; HC, healthy control; m, months; M, male; MCI, mild cognitive impairment; miRNA, microRNA; MMSE, mini-mental state examination; NI, no information; PiB-SUVR, Carbon-11-labelled Pittsburgh compound B-standardised uptake value ratio. Positive APOE $\epsilon 4$ is indicated by '+'. Negative for APOE $\epsilon 4$ is indicated as '-'. A β burden was expressed as PiB-SUVR. Participants who presented with a low A β burden in the brain upon ^{11}C -PiB PET neuroimaging have a PiB-SUVR < 1.5. Participants who presented with high A β burden in the brain upon ^{11}C -PiB PET neuroimaging have a PiB-SUVR > 1.5. Please refer to previous study for more details on PiB-SUVR.² Clinical classification at baseline and 54 months is diagnosed by NINCDS-ADRDA criteria for AD. Classification obtained using AD associated miRNA exosomal biomarkers during the validation study are indicated under miRNA classification.

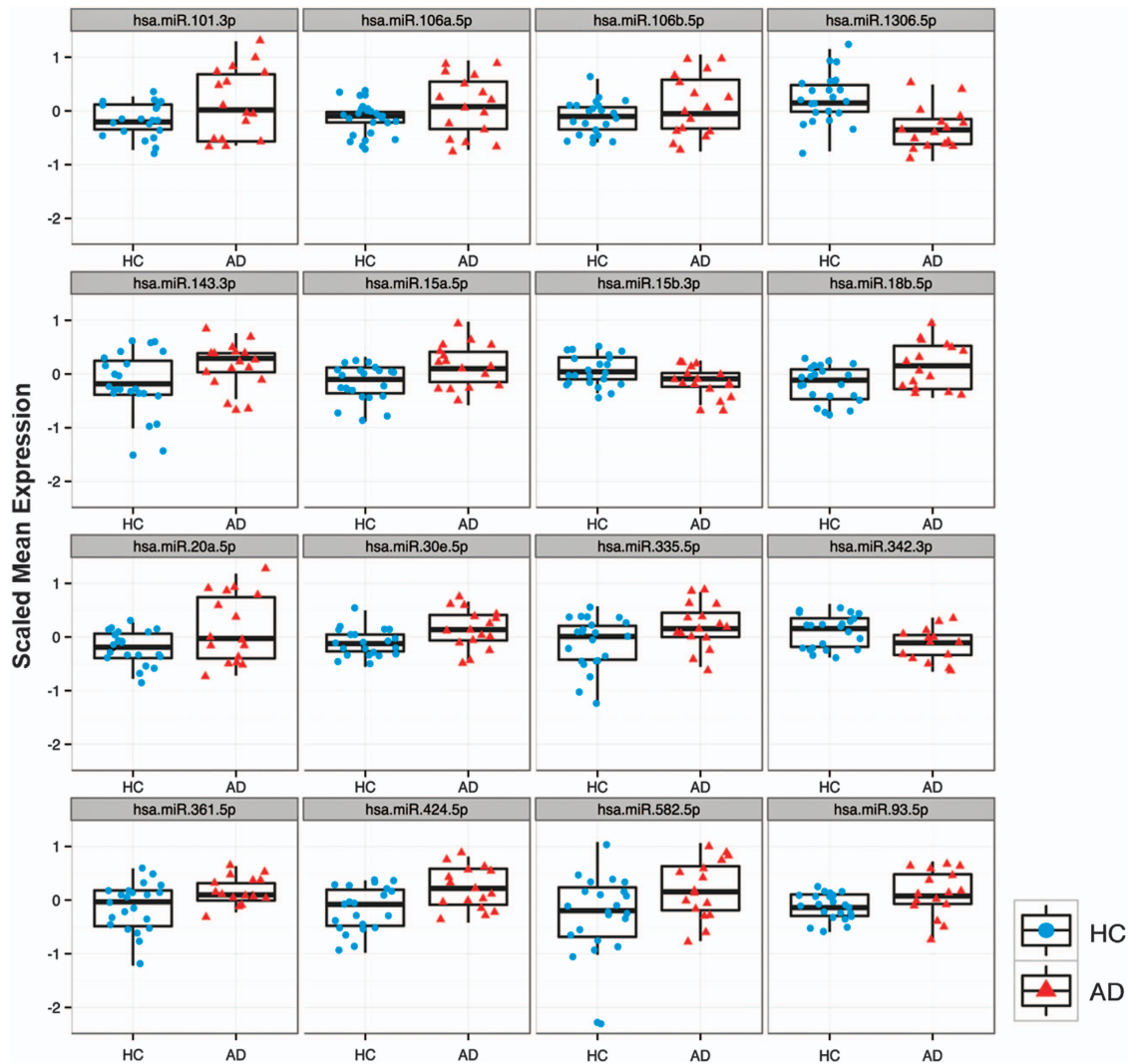


Figure 3. Box plots showing validated microRNA differentially expressed in healthy controls (HC) and participants with Alzheimer's disease (AD). Mean centred and scaled data were plotted between HC and AD participants. HC participants are represented by blue circular dots, whereas AD participants are represented by red triangular dots.

APP levels and the accumulation of A β in human cell lines and hippocampal neurones.^{31,32} The miR-15 family has been observed to regulate Tau phosphorylation through ERK1 leading to neuronal death in Neuro2a cells and primary cortical neurones.³³ miR-424-5p shares the same seed sequence as miR-15, thus belonging to the same miR-15 family of miRNAs.³⁴ Hsa-miR-1306 was predicted to target the 3' untranslated region of α -secretase (ADAM10; a disintegrin and metalloproteinase 10), responsible for the generation of secreted APP.³⁵ The regulation of ADAM10 by hsa-miR-1306 was demonstrated in SH-SY5Y cells expressing the 3' untranslated region of ADAM10 under a luciferase reporting vector, whereby hsa-miR-1306 lowered luminescent signal to 72% compared with control cells.³⁵ Impairment of cellular cholesterol efflux through suppression of ATP-binding cassette transporter A1 (ABCA1) by hsa-miR-106 was demonstrated to result with increased A β secretion.³⁶ In addition, the downregulation of hsa-miR-106b in APP^{swe}/PS Δ E9 mice was found to influence transforming growth factor- β signalling that has a role in neuroprotection.³⁷ Significantly, the majority of these miRNA have also been detected in studies involving deep sequencing strategies of brain tissue.^{38,39}

We detected a large coverage of miRNA extracted from exosomal serum samples isolated for AD biomarker discovery by NGS. The advantage of NGS is its ability to detect absolute counts of all miRNA present in samples. However, in order to successfully validate miRNA assays by qRT-PCR technology for diagnostic assays, miRNA expression needs to reach the threshold of qRT-PCR detection. Using the deep sequencing workflow performed in this study, we estimate ~ 50 reads per million must be obtained across the majority of biological samples for successful biomarker validation by qRT-PCR. From the 1419 mapped miRNA identified in this cohort, 220 highly abundant miRNA were present in all samples across the study. The discovery set revealed 17 significantly differentially expressed exosomal miRNA in AD participants. Upon validation by qRT-PCR, 16-miRNA were successfully detected and displayed consistent miRNA expression changes within AD participants when compared with expression changes detected by NGS. The commonly used comparative delta delta C_t approach ($\Delta\Delta C_t$) in qRT-PCR may not be applicable for diagnostic use as a HC group is required for every run. Therefore, we have applied normalised ΔC_t into a Random Forest model to predict clinical classification. Such a model was able to predict

clinical classification (at time of collection) with high accuracy (87% sensitivity and 77% specificity).

Interestingly, the participant with the highest PiB-SUVr score of 3.03 was not detected as AD using miRNA biomarkers. This highlights a possible limitation in the ability to diagnose those with late AD, and supports the notion that the rate of pathogenesis, in particular A β deposition, slows in the later stages of AD when patients experience cerebral atrophy and severe cognitive impairment.² Participants in the AIBL study were diagnosed according to NINCDS-ADRDA criteria, which are heavily reliant on cognitive and neuropsychological testing for a clinical diagnosis of probable AD. Thus, in this study, we have compared the diagnosis obtained by miRNA analysis with the participant's classification by NINCDS-ADRDA criteria. Although a possible limitation of this study is the small sample size in both discovery and validation cohorts, we demonstrate particular strength of the classifications using the longitudinal strength of the PiB-PET neuroimaging data.

Furthermore, the additional strength of this study comes from the extensive database of metadata collected at baseline through to 54 months. Each participant underwent a battery of assessment including APOE ϵ 4 genotyping, cognitive examination and A β neuroimaging. A β neuroimaging and APOE ϵ 4 genotyping information for those clinical healthy participants classified with AD in this study suggested a higher risk of progression towards AD. Longitudinal studies performed by the AIBL group have also shown that HC subjects with a positive A β scan are of significant risk.⁴⁰ These participants will be carefully monitored in future time points. Taking into consideration that these HC participants could actually be preclinical AD, the predicted specificity would increase to 91.4%.

Owing to the significant involvement of A β and pTau in the pathogenesis of AD, biomarker studies have been largely focused on the detection of insoluble A β and pTau in CSF.^{41,42} Interestingly, hsa-miR-27a-3p was found to be downregulated in CSF of AD patients who also displayed high CSF total tau, CSF pTau and low CSF A β .⁴³ Although these CSF biomarkers have shown high accuracy for confirmation of clinical diagnosis, the collection of CSF is an invasive method requiring highly trained personnel to perform a high-risk lumbar puncture. Large variations in CSF biomarker measurements have been observed between studies, and between and within laboratories, thus CSF testing would need to be centralised.⁴⁴ Longitudinal cohort studies such as AIBL and Alzheimer's Disease Neuroimaging Initiative have demonstrated that A β neuroimaging is able to detect abnormal A β deposition ~20 years before A β reaches the level observed in AD.² Other promising biomarkers of AD involve metabolomics and lipidomics profiling, whereby a set of 10 lipids and metabolites from plasma was found to predict conversion to MCI or AD within a 2–3 year time frame with over 90% accuracy.⁴⁵ Furthermore, a panel of plasma proteins have also been identified to classify patients that have progressed to AD with 90% accuracy.⁴⁶ Cognitive assessment, heavily reliant by NINCDS-ADRDA, can be subjective as it can be difficult to differentiate patients with AD from normal cognitive aging. The portfolio of AD biomarkers^{2,42,45,47} including exosomal miRNA biomarkers should work complementary to provide peripheral predictive and screening tools to assist in the early diagnosis of AD.

Ultimately, the objective and purpose of the exosomal miRNA biomarker test is to predict future cognitive decline in asymptomatic individuals and during the progression of patients with early dementia before referring patients to CSF testing or specialised PET brain imaging. Further applications of this test would help improve diagnostic accuracy to enrich patient cohorts and will be critical in the development of disease-modifying or preventive therapies for AD. This study represents a vital step towards developing a cost-effective, non-invasive and low-risk diagnostic

test to detect the onset and monitor the various stages of AD in order for physicians to provide optimal care for patients.

CONFLICT OF INTEREST

The authors declare no conflict of interest.

ACKNOWLEDGMENTS

This work was supported by the National Health and Medical Research Council (628946 to AFH and CLM) and project grants from The Judith Jane Mason and Harold Stannett Williams Memorial Foundation and Alzheimer's Australia (to LC and AFH). LC was supported by a University of Melbourne Early Career Researcher Project Grant for the work and AFH is an Australian Research Council Future Fellow (FT100100560 to AFH). This work was also supported in part by the NHMRC project grant 1071430 to VLV and VLV is supported by an NHMRC Senior Research Fellowship. AIBL was supported by the Science Industry and Endowment Fund (sief.org.au), the McCusker Alzheimer's Research Foundation and the National Health and Medical Research Council via the Dementia Collaborative Research Centres program (DCRC2).

REFERENCES

- Cole SL, Vassar R. The role of amyloid precursor protein processing by BACE1, the beta-secretase, in Alzheimer disease pathophysiology. *J Biol Chem* 2008; **283**: 29621–29625.
- Villemagne VL, Burnham S, Bourgeat P, Brown B, Ellis KA, Salvado O et al. Amyloid deposition, neurodegeneration, and cognitive decline in sporadic Alzheimer's disease: a prospective cohort study. *Lancet Neurol* 2013; **12**: 357–367.
- Hansson O, Zetterberg H, Buchhave P, Londos E, Blennow K, Minthon L. Association between CSF biomarkers and incipient Alzheimer's disease in patients with mild cognitive impairment: a follow-up study. *Lancet Neurol* 2006; **5**: 228–234.
- Krol J, Loedige I, Filipowicz W. The widespread regulation of microRNA biogenesis, function and decay. *Nat Rev Genet* 2010; **11**: 597–610.
- He L, Hannon GJ. MicroRNAs: small RNAs with a big role in gene regulation. *Nat Rev Genet* 2004; **5**: 522–531.
- Valadi H, Ekstrom K, Bossios A, Sjostrand M, Lee JJ, Lotvall JO. Exosome-mediated transfer of mRNAs and microRNAs is a novel mechanism of genetic exchange between cells. *Nat Cell Biol* 2007; **9**: 654–659.
- Mitchell PS, Parkin RK, Kroh EM, Fritz BR, Wyman SK, Pogosova-Agadjanyan EL et al. Circulating microRNAs as stable blood-based markers for cancer detection. *Proc Natl Acad Sci USA* 2008; **105**: 10513–10518.
- Bellingham SA, Guo BB, Coleman BM, Hill AF. Exosomes: vehicles for the transfer of toxic proteins associated with neurodegenerative diseases? *Front Physiol* 2012; **3**: 124.
- Skog J, Wurdinger T, van Rijn S, Meijer DH, Gainche L, Sena-Esteves M et al. Glioblastoma microvesicles transport RNA and proteins that promote tumour growth and provide diagnostic biomarkers. *Nat Cell Biol* 2008; **10**: 1470–1476.
- Hunter MP, Ismail N, Zhang X, Aguda BD, Lee EJ, Yu L et al. Detection of microRNA expression in human peripheral blood microvesicles. *PLoS ONE* 2008; **3**: e3694.
- Cheng L, Sharples RA, Scicluna BJ, Hill AF. Exosomes provide a protective and enriched source of miRNA for biomarker profiling compared to intracellular and cell-free blood. *J Extracell Vesicles* 2014; **3**. doi:10.3402/jev.v3.23743 (e-pub ahead of print)
- Cheng L, Quek CY, Sun X, Bellingham SA, Hill AF. The detection of microRNA associated with Alzheimer's disease in biological fluids using next-generation sequencing technologies. *Front Genet* 2013; **4**: 150.
- Coleman BM, Hanssen E, Lawson VA, Hill AF. Prion-infected cells regulate the release of exosomes with distinct ultrastructural features. *FASEB J* 2012; **26**: 4160–4173.
- Rowe CC, Ellis KA, Rimajova M, Bourgeat P, Pike KE, Jones G et al. Amyloid imaging results from the Australian Imaging, Biomarkers and Lifestyle (AIBL) study of aging. *Neurobiol Aging* 2010; **31**: 1275–1283.
- Ellis KA, Rowe CC, Villemagne VL, Martins RN, Masters CL, Salvado O et al. Addressing population aging and Alzheimer's disease through the Australian imaging biomarkers and lifestyle study: collaboration with the Alzheimer's Disease Neuroimaging Initiative. *Alzheimers Dement* 2010; **6**: 291–296.
- Ellis KA, Bush AI, Darby D, De Fazio D, Foster J, Hudson P et al. The Australian Imaging, Biomarkers and Lifestyle (AIBL) study of aging: methodology and baseline characteristics of 1112 individuals recruited for a longitudinal study of Alzheimer's disease. *Int Psychogeriatr* 2009; **21**: 672–687.
- McKhann G, Drachman D, Folstein M, Katzman R, Price D, Stadlan EM. Clinical diagnosis of Alzheimer's disease: report of the NINCDS-ADRDA Work Group under the auspices of Department of Health and Human Services Task Force on Alzheimer's Disease. *Neurology* 1984; **34**: 939–944.

- 18 Cheng L, Sun X, Scicluna BJ, Coleman BM, Hill AF. Characterization and deep sequencing analysis of exosomal and non-exosomal miRNA in human urine. *Kidney Int* 2013; **86**: 433–444.
- 19 Vandesompele J, De Preter K, Pattyn F, Poppe B, Van Roy N, De Paepe A *et al*. Accurate normalization of real-time quantitative RT-PCR data by geometric averaging of multiple internal control genes. *Genome Biol* 2002; **3**: 34.
- 20 Kirschner MB, Edelman JJ, Kao SC, Vallely MP, van Zandwijk N, Reid G. The impact of hemolysis on cell-free microRNA biomarkers. *Front Genet* 2013; **4**: 94.
- 21 Haqqani AS, Delaney CE, Tremblay TL, Sodja C, Sandhu JK, Stanimirovic DB. Method for isolation and molecular characterization of extracellular microvesicles released from brain endothelial cells. *Fluids Barriers CNS* 2013; **10**: 4.
- 22 Huang X, Yuan T, Tschannen M, Sun Z, Jacob H, Du M *et al*. Characterization of human plasma-derived exosomal RNAs by deep sequencing. *BMC Genomics* 2013; **14**: 319.
- 23 Gibbings DJ, Ciaudo C, Erhardt M, Voinnet O. Multivesicular bodies associate with components of miRNA effector complexes and modulate miRNA activity. *Nat Cell Biol* 2009; **11**: 1143–1149.
- 24 Mitchell JP, Court J, Mason MD, Tabi Z, Clayton A. Increased exosome production from tumour cell cultures using the Integra CELLine Culture System. *J Immunol Methods* 2008; **335**: 98–105.
- 25 Leidinger P, Backes C, Deutscher S, Schmitt K, Mueller SC, Frese K *et al*. A blood based 12-miRNA signature of Alzheimer disease patients. *Genome Biol* 2013; **14**: R78.
- 26 Kumar P, Dezsó Z, MacKenzie C, Oestreicher J, Agoulnik S, Byrne M *et al*. Circulating miRNA biomarkers for Alzheimer's disease. *PLoS ONE* 2013; **8**: e69807.
- 27 Villarroya-Beltrí C, Gutierrez-Vazquez C, Sanchez-Cabo F, Perez-Hernandez D, Vazquez J, Martín-Cofreces N *et al*. Sumoylated hnRNPA2B1 controls the sorting of miRNAs into exosomes through binding to specific motifs. *Nat Commun* 2013; **4**: 2980.
- 28 Vella LJ, Sharples RA, Lawson VA, Masters CL, Cappai R, Hill AF. Packaging of prions into exosomes is associated with a novel pathway of PrP processing. *J Pathol* 2007; **211**: 582–590.
- 29 Sharples RA, Vella LJ, Nisbet RM, Naylor R, Perez K, Barnham KJ *et al*. Inhibition of gamma-secretase causes increased secretion of amyloid precursor protein C-terminal fragments in association with exosomes. *FASEB J* 2008; **22**: 1469–1478.
- 30 Bellingham SA, Coleman BM, Hill AF. Small RNA deep sequencing reveals a distinct miRNA signature released in exosomes from prion-infected neuronal cells. *Nucleic Acids Res* 2012; **40**: 10937–10949.
- 31 Long JM, Lahiri DK. MicroRNA-101 downregulates Alzheimer's amyloid-beta precursor protein levels in human cell cultures and is differentially expressed. *Biochem Biophys Res Commun* 2011; **404**: 889–895.
- 32 Vilardo E, Barbato C, Ciotti M, Cogoni C, Ruberti F. MicroRNA-101 regulates amyloid precursor protein expression in hippocampal neurons. *J Biol Chem* 2010; **285**: 18344–18351.
- 33 Hebert SS, Papadopoulou AS, Smith P, Galas MC, Planel E, Silahatoglu AN *et al*. Genetic ablation of Dicer in adult forebrain neurons results in abnormal tau hyper-phosphorylation and neurodegeneration. *Hum Mol Genet* 2010; **19**: 3959–3969.
- 34 Finnerty JR, Wang WX, Hebert SS, Wilfred BR, Mao G, Nelson PT. The miR-15/107 group of microRNA genes: evolutionary biology, cellular functions, and roles in human diseases. *J Mol Biol* 2010; **402**: 491–509.
- 35 Augustin R, Endres K, Reinhardt S, Kuhn PH, Lichtenthaler SF, Hansen J *et al*. Computational identification and experimental validation of microRNAs binding to the Alzheimer-related gene ADAM10. *BMC Med Genet* 2012; **13**: 35.
- 36 Kim J, Yoon H, Ramirez CM, Lee SM, Hoe HS, Fernandez-Hernando C. MiR-106b impairs cholesterol efflux and increases Abeta levels by repressing ABCA1 expression. *Exp Neurol* 2012; **235**: 476–483.
- 37 Wang H, Liu J, Zong Y, Xu Y, Deng W, Zhu H *et al*. miR-106b aberrantly expressed in a double transgenic mouse model for Alzheimer's disease targets TGF-beta type II receptor. *Brain Res* 2010; **1357**: 166–174.
- 38 Wang WX, Huang Q, Hu Y, Stromberg AJ, Nelson PT. Patterns of microRNA expression in normal and early Alzheimer's disease human temporal cortex: white matter versus gray matter. *Acta Neuropathol* 2011; **121**: 193–205.
- 39 Cogswell JP, Ward J, Taylor IA, Waters M, Shi Y, Cannon B *et al*. Identification of miRNA changes in Alzheimer's disease brain and CSF yields putative biomarkers and insights into disease pathways. *J Alzheimer's Dis* 2008; **14**: 27–41.
- 40 Rowe CC, Bourgeat P, Ellis KA, Brown B, Lim YY, Mulligan R *et al*. Predicting Alzheimer disease with beta-amyloid imaging: results from the Australian imaging, biomarkers, and lifestyle study of ageing. *Ann Neurol* 2013; **74**: 905–913.
- 41 Blennow K, Hampel H, Weiner M, Zetterberg H. Cerebrospinal fluid and plasma biomarkers in Alzheimer disease. *Nat Rev Neurol* 2010; **6**: 131–144.
- 42 Andreasen N, Minthon L, Davidsson P, Vanmechelen E, Vanderstichele H, Winblad B *et al*. Evaluation of CSF-tau and CSF-Abeta42 as diagnostic markers for Alzheimer disease in clinical practice. *Arch Neurol* 2001; **58**: 373–379.
- 43 Sala Frigerio C, Lau P, Salta E, Tournoy J, Bossers K, Vandenbergh R *et al*. Reduced expression of hsa-miR-27a-3p in CSF of patients with Alzheimer disease. *Neurol* 2013; **81**: 2103–2106.
- 44 Mattsson N, Andreasson U, Persson S, Arai H, Batish SD, Bernardini S *et al*. The Alzheimer's Association external quality control program for cerebrospinal fluid biomarkers. *Alzheimer's Dement* 2011; **7**: 386–395 e386.
- 45 Mapstone M, Cheema AK, Fiandaca MS, Zhong X, Mhyre TR, MacArthur LH *et al*. Plasma phospholipids identify antecedent memory impairment in older adults. *Nat Med* 2014; **20**: 415–418.
- 46 Ray S, Britschgi M, Herbert C, Takeda-Uchimura Y, Boxer A, Blennow K *et al*. Classification and prediction of clinical Alzheimer's diagnosis based on plasma signaling proteins. *Nat Med* 2007; **13**: 1359–1362.
- 47 Rembach A, Watt AD, Wilson WJ, Villemagne VL, Burnham SC, Ellis KA *et al*. Plasma amyloid-beta levels are significantly associated with a transition toward Alzheimer's disease as measured by cognitive decline and change in neocortical amyloid burden. *J Alzheimer's Dis* 2014; **40**: 95–104.

Supplementary Information accompanies the paper on the Molecular Psychiatry website (<http://www.nature.com/mp>)